Cigarette smoke and tumor micro-environment co-promote aggressiveness of human breast cancer cells

Louise Benoit, Celine Tomkiewicz, Maxime Delit, Hanna Khider, Karine Audouze, Flavie Kowandy, Sylvie Bortoli, Robert Barouki, Xavier Coumoul, Meriem Koual

Cigarette smoke and tumor micro-environment co-promote aggressiveness of human breast cancer cells

Louise BENOIT[1,2], Celine TOMKIEWICZ[1], Maxime DELIT[1], Hanna KHIDER[1,2], Karine AUDOUZE[1], Flavie KOWANDY[1], Sylvie BORTOLI[1], Robert BAROUKI[1$], Xavier COUMOUL[1]*, Meriem KOUAL[1,2*$]

*: these authors contributed equally to this work.

[1] Université Paris Cité, T3S, INSERM UMR-S 1124, 45 rue des Saints Pères, Paris, France

[2] Assistance Publique-Hôpitaux de Paris, European Hospital Georges-Pompidou, Gynecologic and Breast Oncologic Surgery Department, Paris, France

[$] Co-corresponding author:

Robert BAROUKI

Université Paris Cité, 45 Rue des Saints-Pères, 75006 Paris

E-mail: robert.barouki@parisdescartes.fr

Tel: 33 (0)1 76 53 43 72,

Meriem KOUAL

European hospital Georges Pompidou, 20 rue Leblanc, 75015 Paris

E-mail: meriem.koual@aphp.fr

Tel: 01 56 09 25 63

Conflict of interest: The authors declare they have nothing to disclose.

Word count: 5539, introduction 608 (max 750), discussion 1275 (max 1500)

Keywords: mammary cancer, metastasis, pollutants, smoking, adipose tissue

Running head: The impact of the environment on breast cancer metastasis

Abstract

Breast cancer is a major public health issue and the role of pollutants in promoting breast cancer progression has recently been suggested. We aimed to assess if a mixture of pollutants, cigarette smoke, could favor the aggressivity of breast cancer cells. We also evaluated the impact of the tumor micro-environment, largely represented by adipocytes, in mediating this modification of cell phenotype.

Breast cancer cells lines MCF-7 were cultured using a transwell coculture model with preadipocytes hMADS cells or were cultured alone. Cells were treated by cigarette smoke extract (CSE) and the four conditions: control, treated by CSE, coculture and coexposure (coculture and CSE) were compared. We analyzed morphological changes, cell migration, resistance to anoikis, stemness, epithelial to mesenchymal transition (EMT) and presence of hormonal receptors in each condition. A complete transcriptomic analysis was carried out to highlight certain pathways. We also assessed whether the aryl hydrocarbon receptor (AhR), a receptor involved in the metabolism of xenobiotics, could mediate these modifications.

Several hallmarks of metastasis were specific to the coexposure condition (cell migration, resistance to anoikis, stemness characterized by CD24/CD44 ratios and ALDH1A1 and ALDH1A3 rates) whereas others (morphological changes, EMT, loss of hormonal receptors) could be seen in the coculture condition and were aggravated by CSE (coexposure). Moreover, MCF-7 cells presented a decrease in hormonal receptors, suggesting an endocrine treatment resistance. These results were confirmed by the transcriptomic analysis. We suggest that the AhR could mediate the loss of hormonal receptor and the increase in cell migration

Introduction

Breast cancer is the leading cause of cancer in women in terms of incidence and mortality (Bray et al. 2018). If the tumor remains localized to its site of appearance, the five-year survival rate is 99%; however, once the cancer spreads to the lymph nodes or at distance (depicted therefore as aggressive), the five-year survival rate drops to 86% and 28%, respectively (Siegel et al. 2021). Many risk factors for the incidence of breast cancer have been found, however, knowledge lacks on the mechanism and the risk factors of metastasis.

The role of the environment has recently been suspected to take part in breast cancer aggressiveness. Indeed, several pollutants have been found to promote breast cancer progression toward a more aggressive phenotype. *In vitro*, the Seveso dioxin (or TCDD, 2,3,7,8-Tetrachlorodibenzo-*p*-dioxin), a pollutant mainly found in high-fat foods (fish, meat, cheese…) could enhance stemness, migration and oxidative stress in breast cancer cells (Lin et al. 2007; Lin et al. 2008; Koual et al. 2021). Likewise, hexachlorobenzene (HCB), a fungicide, could promote angiogenesis (Pontillo et al. 2015; Zárate et al. 2020) and migration *in vitro* (Pontillo et al. 2013; Miret et al. 2016). These compounds are ligands of the aryl hydrocarbon receptor (AhR), a receptor involved in the regulation of xenobiotics metabolism. Recent evidence suggests that the AhR could mediate the impact of the pollutants on breast cancer aggressiveness (Benoit et al. 2022). However, most of these works comprised of two main limitations: i) they failed to take into account the tumor micro-environment, and ii) they studied the impact of a single pollutant and not a mixture of pollutants.

First, the role of the tumor microenvironment appears to be critical in the pathophysiological process of breast cancer metastasis (Paget 1989). The tumor microenvironment of the breast cancer cell mainly consists in adipose cells which could be in part responsible for breast cancer aggressiveness (Blücher and Stadler 2017). Indeed, adipocytes in contact with breast cancer cells can transform into cancer-associated adipocytes (CAA) which provide nutrients to the tumor cells and promote breast cancer aggressiveness triggering chemo-resistance, EMT and invasion (Lee et al. 2015; Lehuédé et al. 2019; Rybinska et al. 2020). Our team has created a coculture model for breast cancer and has already assessed the impact of a dioxin on this model and found that it increased migration, aggressiveness and stemness (Koual et al. 2021).

Second, evaluating the effect of a mixture of pollutants is closer to the 'real life exposure". Yet, *in vitro* studies are scarce. Using a complex mixture containing 15 organochlorines, Aubé et al. found that their cocktail acts differentially on human breast cell lines which were compared according to their status of expression of nuclear receptors (including estrogen receptor-α or ER) (Aubé et al. 2011). The other works evaluated only the estrogenicity of their mixture and not the potential to promote a pro-metastatic phenotype (Rajapakse et al. 2002; Silva et al. 2002). We chose to use cigarette smoke extract as our mixture of pollutants. Indeed, even if the role of smoking in breast cancer incidence is uncertain, it has been suggested in epidemiologic studies, that smokers could have more aggressive breast cancers. These patients have a higher mortality rate (Pierce et al. 2014; Nechuta et al. 2016) and more triple

negative cancers (Cooper et al. 1989; Manjer et al. 2001). Murin et al. even found that smoking patients had more pulmonary metastasis at diagnosis than non-smokers (Murin and Inciardi 2001). *In vitro*, Dicello et al. found that chronic exposure to cigarette smoke could promote epithelial to mesenchymal transition (EMT) in ER-positive breast cancer (Di Cello et al. 2013).

Our goal was to assess the impact of exposure to cigarette smoke extract as a common mixture of pollutants on the promotion of breast cancer metastasis and aggressiveness in these cells cocultured. We hypothesized that the effect was mediated by the AhR. We focused our research on ER-positive breast cancer cells to assesses if these pollutants could indorse an aggressive phenotype to these cells when cocultured with adipocytes. Indeed, this type of breast cancer has the best prognosis and the best response to treatment.

Methods

1) Cell lines

Different cell lines were used; MCF-7 human breast cancer cells (ATCC® HTB-22), a cell line expressing estrogen receptor (ER+) and progesterone receptor (PR+), MDA-MB-231 human breast cancer cells (ATCC® HTB-26), a triple negative cell lines (ER-, PR-, Her2-) and HS-578T human mammary carcinosarcoma cells (ATCC® HTB-126), an ER−/PR−/HER2− cell line. HS-578T AhR-KO cells were generously provided by Dr. David Sherr (Department of Environmental Health, Boston University School of Public Health, 72 East Concord St., Boston, MA 02118, USA) (Stanford et al. 2016; Narasimhan et al. 2018).

Human pre-adipocytes were chosen to represent the tumor micro-environment as previously described (Koual et al. 2021). Briefly, these cells have higher secretory capacities and are a major component of the adipose tissue (Kim et al. 2012; Kothari et al. 2020). They were isolated from human adipose tissue, and they maintain their properties after several passages. The hMADS cell line (human multipotent adipose-derived stem cells) has been described previously and was provided by Christian Dani (Institut de Biologie Valrose/Université Côte d'Azur, UMR CNRS/INSERM, Faculté de Médecine, Nice, France) (Rodriguez et al. 2005).

Details concerning cell lines are presented in the Supplementary Material and Methods

2) The Coculture Model (Koual et al. 2021)

MCF-7 cells and hMADS preadipocytes were cocultured in transwell culture plates in hMADS medium without hFGF2. Briefly, 400,000 MCF-7 cells were seeded into the lower well, and 200,000 hMADS preadipocyte cells were seeded onto polyester membrane inserts (0.4 µm pore size - Sarstedt,

Nürnbrecht, Germany) on the upper part in 6-well culture dishes. The two cell types shared the same culture medium, which diffuses through the inserts. MCF-7 cells also were grown alone as controls. After 24 h of incubation at 37°C, the medium was replaced, and the cells were exposed to 1% cigarette smoke extract (CSE) for 48 h. In the rest of the document, the condition "MCF-7 cells grown in the presence of the hMADS cells" is called "coculture," and the condition "MCF-7 grown in the presence of the hMADS cells treated with the CSE" is called "coexposure" (which also correspond to a coculture condition treated with CSE).

3) Aqueous Cigarette smoke extract (CSE)

Cigarette smoke was extracted from filtered mainstream smoke from a reference brand (1R6F research cigarettes; Tobacco Health Research, Lexington, KY) generously provided by Dr. Sophie Lanone (IMRB, Mondor, France) (Jaccard et al. 2019). We prepared the aqueous cigarette smoke extract (CSE) as previously described with some modifications (Baskara et al. 2020). The whole protocol is detailed in the Supplementary Material and methods and represented Figure 1. Moreover, the choice of the dose and the duration is described in the Supplementary data and in Supplemental Figure S1.

4) Migration assay

Two types of migration tests were used: 1) the Boyden chamber assay and 2) the xCELLigence migration assay. Indeed, MCF-7 cells migrate slower than the triple-negative cell lines (HS-578T and MDA-MB 231 cells), and the Boyden chamber assay was found more accurate to measure subtle changes of the first cell line. To summarize, a Boyden chamber assay was used to study MCF-7 migration and an xCELLigence migration assay was used for both triple negative cells.

For the Boyden chamber assay, breast cancer cells lines, MCF-7 were plated in a 6 well plate with 400 000 cells per well with or without coculture (200 000 hMADS). After 24 hours, they were treated by CSE 1% for 48 hours. The cells were then trypsinized and plated in 24 well-plate with a Boyden chamber (8 µm-pores Sarstedt, Nürnbrecht, Germany) with two replicates per condition. After trypsinization, cells were not treated again by the CSE. Twelve thousand cells were plated in the upper chamber with 100 µl of medium without serum and 600 µl of medium with 10% serum was put in the lower chamber as a chemoattractant for migrating cells. Four days later, a cotton swab was used to remove non-migrated cells from the upper side of the insert and the membranes were then stained with Hoechst (1µg/mL) and photographed using an ImageXpressPICO device (Molecular devices). The results of the Boyden chamber experiments were obtained from 4 biological replicates.

For both triple negative MDA-MB-231 or HS-578T cells, their fast cell migration was monitored using the xCELLigence RTCA DP instrument (Agilent Technologies). The protocol is detailed in the Supplementary Material and Methods.

5) Anchorage-independent growth in soft agar

To study the cell capacity of surviving in a hostile environment, the resistance to anoikis (or anchorage-independent growth) was quantified using the protocol described by Joussaume *et al* (Joussaume et al. 2020). Breast cancer cells lines, MCF-7 were plated in a 6 well plate with 400 000 cells per well with or without coculture (200 000 hMADS). After 24 hours, they were treated by CSE 1% for 48 hours. The cells were then trypsinized and single-cell suspensions of MCF-7 cells were prepared from monolayer cultures. After trypsinization, cells were not treated again by the CSE. Cells were suspended in culture medium containing 10% FBS and 0.4% soft agar at 37°C and then 2000 cells were plated onto a solidified bottom layer containing culture medium of 10% FBS and 0.6% soft agar. Twenty-eight days later, cells were stained with a 1% Nitrotetrazolium Blue Chloride (NBT) solution, which stains live cells, from Sigma-Aldrich and imaged on a ChemiDoc MP Imaging System (Bio-Rad-France). The number and size of colonies were compared between the conditions using Image-J software (Schneider et al. 2012).

6) Stemness CD24/44 assay

MCF-7 cells were plated in a 6 well-plate with 400 000 cells per well with or without coculture (200 000 hMADS). After 24 hours, they were treated by CSE 1% for 48 hours. The cells were then trypsinized, counted and 200 000 cells were placed in each tube. The cells were stained by BV421-anti CD44 (Bdbiosciences- 562890) and FITC-anti CD24 (Invitrogen-11024742 (1/200)) for 30 minutes on ice and in the dark, washed by PBS and analyzed using cell cytometry (BD Canto II flow cytometer). Both CD24 and CD44 are membrane glycoproteins, and their detection can be performed without permeabilization.

7) Immunofluorescent Staining

MCF-7 cells were plated in a 6 well-plate with 400 000 cells per well with or without coculture (200 000 hMADS) and onto coverslips. After 24 hours, they were treated by CSE 1% for 48 hours. The cells were then fixed with 4 % paraformaldehyde for 20 min and permeabilized with 0.2 % Triton X-100 for 3 min at room temperature, then washed with PBS. The cells were incubated in a blocking solution (0.3 M PBS-Glycin -1% bovine serum albumin) for 1h and then incubated with the primary antibody (Paxillin – ab32084- Abcam) in PBS for 1h30 min at room temperature. After washing with PBS-T (PBS containing 0.1 % Tween-20), the cells were incubated with a second antibody conjugated with a fluorescent dye for 1h at room temperature. For the staining of actin and nuclei, FITC-conjugated

phalloidin and TO-PRO-3 (Invitrogen) were included during the incubation with the secondary antibody. The coverslips were sealed with Dako Faramount Aqueous Mounting Medium Ready-to-use (Invitrogen) and images were recorded using a Zeiss LSM 510 confocal microscope (Carl Zeiss Meditec France SAS, Le Pecq, France) using a 40X Plan-Neofluar 1.3 NA oil objective and Zen Blue software (Zeiss).

Details concerning antibodies can be found in the Supplementary Table 1.

8) Proliferation assays

MCF-7 cells were plated in a 6 well-plate with 400 000 cells per well with or without coculture (200 000 hMADS). After 24 hours, they were treated by CSE 1%. Since MCF-7 cells proliferate slowly, proliferation was assessed on day 4 or 6 and proliferation was assessed either with a Click Proliferation Kit or a CFSE assay. Protocols are detailed in the Supplementary Material and Methods.

9) Western blot

Protein extraction was performed after 48 hours of treatment (control, CSE, coculture and coexposure). Briefly, MCF-7 cells were lysed in the 6-well plate with the RIPA lysis buffer (Radio-Immunoprecipitation assay buffer, Sigma-Aldrich ®) for 1 hour at 4°C. They were then scratched and stored at -20°C. Protein concentrations were assessed using a Micro BCA™ Assay Kit and the plate were read using a spectrophotometer (560 nm).

Samples were adjusted to 10 ug of proteins and boiled for 5 minutes. They were then resolved by electrophoresis on 10**%** polyacrylamide gels (Mini-protean ® TGX, Bio Rad ®) and transferred to nitrocellulose membranes (Trans-blot ® Turbo™, Biorad®). Non-specific proteins were blocked by incubating membranes in PBS 1X with 5% ECL (electrochemiluminescence) powder for one hour.

Immunoblots were incubated with primary antibodies anti-E-α (Santa Cruz 543, d 1:1000), anti-PR (abcam 2765, d 1:1000), actin (ab 8227, 1:3000) and subsequently, appropriate secondary anti-rabbit (d 1:1000) or anti-mouse (d 1:2000) antibodies (Cell Signaling Technology®, #7074S and #7076S respectively).

Blots were revealed using chemiluminescence technique (ECL western blotting substrate, Pierce ®) with Fusion Solo S imager (Vilber ®). For quantification, specific bands were normalized to their actin level and then compared to the non-treated condition.

10) Modulation of the expression or activity of the AhR (Knock-out, and agonist)

AhR KO: HS-578T cells (ATCC® HTB-126), a triple negative human mammary carcinosarcoma cell line with also a KO for the AhR were used as previously described (Stanford et al. 2016; Narasimhan et al. 2018).

AhR agonist: TCDD (#ED-901, CAS: 1746-01-6) was purchased from LGC Standards, and nonane was purchased from Sigma-Aldrich. The TCDD stock solution at 155 µM in nonane (100%) was diluted at 25 nM (0.016%) in the culture medium before treating the cells. After 24 h of coculture, the medium was replaced, and the cells were treated with 25 nM TCDD or vehicle for 48 h (for a total of 72 h after seeding).

11) Total RNA extraction and samples

MCF-7 cells were plated in a 6-well plate with 400 000 cells per well with or without coculture (200 000 hMADS). After 24 hours, the plates were exposed to CSE 1% for 48 hours. Total RNA of MCF-7 cells was extracted using a RNeasy Plus Mini kit (Qiagen). The samples were stored at -80°C. The concentrations and ratios A260/A280nm and A260/A230nm for RNA purity analysis were measured with a Nanodrop One (Ozyme ®).

12) *Reverse transcription quantitative PCR (qRT-PCR).*

Reverse transcription was performed using the high-capacity cDNA reverse transcription Kit (Applied Biosystems ®) as described. Then quantitative PCR was performed using 20 ng of cDNA per reaction on CFX 384 thermocycler (Bio-Rad®). Duplicated reactions of each sample were performed using Takyon SYBR® 2X qPCR Mastermix Blue (Eurogentec ®).
The human primers are detailed Supplementary Table 2**.** The relative amounts of mRNA were estimated compared with the control condition using the ΔΔCt method with RPL13A RNA as the reference. Data are representative of at least three different experiments and are expressed as the mean ± SD (Standard Deviation).

13) Transcriptomic analysis: RNA sequencing

A complete RNA sequencing was also carried out. The 4 conditions of exposure (control, CSE, coculture, coexposure) were analyzed and transcriptomic analysis was performed on 5 biological replicates to eliminate a batch effect.
RNA sequencing and analysis was carried out with the help of the GENOMI'C Platform (UDP-8104, Dr Frank Letourneur, University Paris Cité, Cochin institute, 75014 Paris) and is detailed in the Supplementary Material and Methods.

14) Statistical analysis

Each experiment was performed at least in triplicate. The results of three or more independent experiments are expressed as the mean ± SD. Statistical analysis was performed with GraphPad Prism software using Kruskal–Wallis's H test (nonparametric comparison of *k* independent series) followed by a 1-factor analysis of variance (parametric comparison of *k* independent series). Due to the small size of our samples, we could not hypothesize a normal distribution. A value of $p<0.05$ was considered statistically significant: * $p<0.05$ **, $p<0.01$, *** $p<0.001$ and **** $p<0.0001$.

Results

Coculture and to a greater extent, coexposure, modify the cell morphology of breast cancer cells with the presence of giant cells and 'cell-in-cell' structures.

Immunofluorescence staining was performed to evaluate the morphological changes on MCF-7 cells under the different conditions of culture. Antibodies against paxillin were used to examine the focal adhesion sites and the staining of actin with FITC-conjugated phalloidin was used to visualize rearrangements of the cytoskeleton (Figure 2A). Control MCF-7 cells are jointed, rather small and paxillin is located in the cytoplasm. After treatment by CSE, the cells dissociated with a star-like morphology and paxillin relocated to the ends of the membrane extensions allowing to visualize the cell anchor points. In the coculture condition, several cells were much larger with an extended nuclei and lamellipodia (defined as membrane extensions composed of actin polymers that the cell uses to move within the extracellular matrix) appeared. In the coexposure condition, the morphology of cells is dramatically changed with 1) paxillin localized both in the membrane extensions and in the cytoplasm, 2) large, dissociated, star-shaped and sometimes even plurinucleated cells. These large polynuclear giant cells are evocative of cell-in-cell structures, a significant marker of either entosis or cellular cannibalism (M et al. 2007; Krishna and Overholtzer 2016) (Figure 2A). Entosis is defined as the invasion of one cell into another resulting either in its degradation or liberation with a discussed role in cancer promotion. Cell cannibalism results necessarily in the death of the absorbed cell. These findings were noted in both ER-positive and triple negative cells lines (Supplementary Figure S2).

To further explore the cell-in-cell structures, a Ki67 staining was carried out. Antibodies against Ki67 are used to explore cell proliferation since this no-histone nuclear protein is present only during active phases of the cell cycle (G1, S, G2, and mitosis). The internalized engulfed cells are KI67 negative and thus in a state of quiescence, while the engulfing cell is KI67 positive (Figure 2B and Supplementary Figure S2). This could suggest that the latter cell extracts nutrients from the engulfed cell which may therefore constitute a marker of poor prognosis.

The coexposure triggers migration of breast cancer cells.

A migration assay was carried out on the different cancer cell lines. Due to the slow migratory phenotype of the ER-positive MCF-7 cell line, a Boyden chamber assay was performed for these cells and analysis and interpretation of the results were performed after 4 days of migration. While proliferation, assessed in parallel, was not affected by the different treatments (Supplementary Figure S4), only the coexposure condition significantly increased the migration properties of cells (Figure 3A). No increase in migration was found using the CSE alone or under the coculture condition only.

Similar results were found for the triple negative breast cancer MD1-MB-231 cells: for these fast-migrating breast cell line (migration is initiated in the first 24h of culture), a xCELLligence assay was carried out with a real time analysis of migration (Supplementary Figure S5).

Both coculture and coexposure conditions promote an epithelial to mesenchymal transition (EMT) in ER-positive cell breast cancer cells.

The results showing significant changes of the migratory and morphological phenotypes observed upon the coexposure condition, evoked a possible EMT mechanism which is defined as the switch from a polarized epithelial cell phenotype to a mesenchymal phenotype with enhanced migratory properties. Three criteria are required to define an EMT: a decrease of epithelial markers, an increase of mesenchymal markers and an enhanced migration (Kalluri and Weinberg 2009).

First, using immunochemistry and confocal microscopy, we noted that, in non-treated cells, E-cadherin, an epithelial marker involved in cell junctions (Kalluri and Weinberg 2009), was localized at cell junctions, suggesting that the cells were well joined together. The co-exposed cells displayed a loss of E-cadherin localization close to the membrane. After treatment by CSE, E-cadherin tends to diffuse in the cytoplasm of the cell. In coculture condition, E-cadherin was mainly localized at cell-cell junctions but also in the cytoplasm of large cells. However, in coexposure conditions, the E-cadherin was completely internalized with the loss of cell junctions (Figure 2C).

Second, we assessed the presence of genes involved in the transformation to a mesenchymal phenotype by qPCR. In accordance with our immunofluorescence findings, *E-cadherin* was gradually decreased in the CSE (fold change 0.75 $p<0.01$), coculture (fold change 0.6, $p<0.0001$) and coexposure conditions (fold change 0.5, $p<0.0001$). *Zeb1*(fold change 2.5, $p<0.0001$) and Twist (fold change 2.2) were only increased in the coexposure condition whereas *Snail* (fold change 1.7 and $p< 0.001$ for coculture and fold change 1.9 $p<0.0001$ for coexposure) and *Slug* (fold change 1.6 and $p< 0.05$ for coculture and fold change 1.5 $p<0.05$ for coexposure) were increased in both coculture and coexposure conditions.

Not all markers are affected by the coexposure condition. *Tgfβ-2*, a profibrotic factor, was increased only in the coculture condition (fold change 3, $p<0.01$) (Figure 4). *Vimentin* and *Fibronectin* were not modified in our different conditions (Supplementary Figure S6).

In conclusion, while the CSE affected several EMT markers, most markers were similarly and significantly altered by the coculture and coexposure condition. However, cell migration was only

significantly increased in the coexposure condition suggesting that EMT is specifically triggered by this condition.

The coexposure promotes stemness in ER-positive MCF-7 breast cancer cells

Stemness is defined as the capacity of a cell to self-renew and to differentiate into diverse cell types. Cancer stem cells are believed to promote both resistance to treatment and distant metastasis through their capacity of survival (Borovski et al. 2011). CD24 (heat stable antigen) and CD44 (hyaluronic acid receptor) are surface glycoproteic markers of cancer stem cells (Li et al. 2017). Their expression is positively associated with breast cancer metastasis (Abraham et al. 2005). When compared to control cells, only the coexposure condition significantly increased the percentage of either CD24+ cells or CD44+ cells (Figure 5A). This was caused mainly by a decrease of the proportion of CD24- /CD44- cells (Supplementary Figure S7).

ALDH1A1 (Aldehyde Dehydrogenase 1 Family Member A1) and ALDH1A3 (Aldehyde Dehydrogenase 1 Family Member A3) are also markers of stemness and involved in poor prognosis (Ginestier et al. 2007). Both CSE and coculture alone significantly enhanced the expression of ALDH1A1 and ALDH1A3 in MCF-7 cells (less than 2-fold, $p<0.05$), yet coexposure further increased ALDH1A3 and ALDH1A1 3-fold ($p<0.0001$) (Figure 5B).

The coexposure increases the resistance to the anoikis in ER-positive MCF-7 breast cancer cells

The acquisition of stemness confers a greater autonomy to the cells in terms of differentiation but also in relation to their microenvironment. Anoikis is defined as a natural process in which cell death occurs after the loss of cell adherence to the extracellular matrix (Joussaume et al. 2020). Certain cancer cells can develop resistance to anoikis through a complex mechanism, promoting invasiveness, resistance to treatment and metastasis (Paoli et al. 2013; Adeshakin et al. 2021). Cell resistance to anoikis is essential to the formation of metastasis since it promotes cell capacity to survive in non-adherent conditions (e.g., blood) and possibly to re-attach elsewhere. An anchorage-independent growth assay in soft agar was used to study resistance to anoikis. MCF-7 cells showed a resistance to anoikis with an increase in both colony number and size only in the coexposure condition (Figure 6). This can therefore suggest an aggressive cell phenotype and a resistance to chemotherapy.

Cigarette smoke extract reduces the expression of hormonal receptors in ER-positive MCF-7 lines in coculture and more importantly, in coexposure conditions

The acquisition of a resistance to anoikis led us to test additional aggressive properties commonly observed at the clinical level such as the loss of nuclear receptors (e.g., estrogen and progesterone receptors). RTqPCR analysis showed that cells treated by CSE, coculture and coexposure conditions presented a gradual decrease in expression of Er-α and PR, since Er-β expression did not change (Figure 7A). The mRNA changes were confirmed by analysis of protein levels; likewise, we found a significant

decrease of the long isoform Er-α protein (66kDa) after Western blot analysis in the coexposure condition (Figure 7B). This loss of one estrogen receptor in our model under coexposure condition, is reminiscent of what is observed clinically as part of the triple negative phenotype (with a worse prognosis and a resistance to endocrine therapy). Full blots can be found Supplemental Figure S8 et S9.

RNA sequencing

A complete transcriptomic analysis was carried out to explore the different pathways triggered by our conditions (Figure 8A). Two hundred and twenty-one (221) genes were differentially regulated (Fold <1.5 or <0.75 and $p<0.05$) by the CSE (control versus CSE), 386 by the coculture condition (control versus coculture) and 345 by CSE in the coculture condition (coculture versus coexposure). Pathways involved in the xenobiotic response and cell motility were upregulated by the CSE alone. Pathways related to the carcinogenic processes (glycolysis, hypoxia, general cancer pathways, neo-angiogenesis and cell motility) were upregulated by the coculture alone. Finally, the coexposure condition increased pathways which are present in both separate conditions such as the xenobiotic responses, drug transport, cancer pathways, estrogen synthesis and cell migration (Figure 8B). Details concerning the enrichments can be found in Supplementary Figures S10-12.

We also analyzed specifically the effect of CSE on MCF-7 cells: 1) CSE vs control; 2) CSE + coculture vs coculture. The presence of the CSE with the coculture specifically upregulated pathways involved in cancer and drug resistance (Figure 8C). To further understand the exploratory analysis of the RNA sequencing, specific qPCRs were carried out on selected drug transporters whose increased expression is a feature of chemoresistance (ABCG2, ABCC2, ALDH1A3, ALDH1A1). The mRNA expression of ABCG2 was increased in both CSE and coexposure conditions and ABCC2 expression was increased by CSE (Supplemental Figure S5). ALDH1A3 and ALDH1A1 mRNA levels, also involved in resistance to treatment, were increased in both CSE and coculture conditions but to a greater extent in the coexposure condition (Figure 5B) (Croker et al. 2017).

Full transcriptomic data can be found online in the repository of the International Nucleotide Sequence Database Collaboration, DNA bank of Japan (ID PSUB018279) and in the Supplementary transcriptomic data (Excel file).

Effects of the AhR on cell migration

Several compounds of the CSE are AhR ligands including polycyclic aromatic hydrocarbons (such as benzo(a)pyrene). We, therefore, carried out a migration assay using two versions of a triple negative breast cancer cell line: HS-578T Cas9 (control or wild-type) and AhR-KO cells. Using the xCELLigence system, we observed a significant increase in cell migration, only in the coexposure condition of the HS-578T Cas 9 cells. This result was in line with those of the MCF-7 cells. In AhR KO cells, both coculture and coexposure led to a similar increase of the migratory potential of the cells but with no difference between these two conditions indicating that CSE has no effect per se. This suggested

a complex effect of AhR knockout on the interactions between the breast and pre-adipocytes cells but also indicated that the AhR knockout impairs the effect of CSE in the coexposure condition (Figure 3B and Supplementary Figure S13).

Effects of the AhR on decrease of ER

We found that the CSE could reduce the presence of hormonal receptors in MCF-7 lines in coculture and more importantly, in coexposure conditions. Several compounds of the CSE are ligands of the AhR, we assessed the role of the AhR in this loss of ER using a specific activator of this receptor. We therefore tested a prototypical ligand of the AhR, TCDD (instead of the CSE). qRT-PCR assays showed that TCDD reduced the expression of Er-α mRNA after 48h treatment. The effect of the coculture remains the same. Interestingly, the decrease is more pronounced under the synergistic coexposure (TCDD and coculture) condition. Moreover, unlike for CSE, Er-β was decreased in the coculture and coexposure conditions (Figure 7C). The Western blot analysis showed similar results with a dramatic decrease of the protein long isoform Er-α (66kDa) in the coculture and coexposure conditions (Figure 7D).

Discussion

The present study highlights that cigarette smoke extracts (CSE) could promote a more aggressive phenotype to breast cancer. Indeed, mammary cancer cells cocultured with cells which partly mimic their micro-environment (hMADS sharing properties of fibroblasts and adipocytes) and treated with CSE, displayed several aggressive properties. We studied the ER-positive MCF-7 cell line since ER-positive breast cancers are known to have a better prognosis. Several assays were also validated in MDA-MB-231 and HS-578T cells but were not emphasized here. We showed that MCF-7 cells acquired a "triple negative-like" phenotype (partly characterized by the loss of hormonal receptors) after exposure to CSE in their micro-environnement, evoking a progression toward a more aggressive phenotype. This evolution is marked by an increase in migration, resistance to anoikis, EMT, stemness, and cell in cell structures. Additional hallmarks of metastasis were specific to this coexposure condition (migration, resistance to anoikis, stemness) whereas others (morphological changes, EMT, loss of hormonal receptors) could be seen in the coculture condition and were aggravated by CSE (coexposure). It must be stressed that most of cancer hallmarks were not seen in the CSE condition alone, emphasizing the importance of the coculture model but also suggesting that the CSE is a sensitizing factor.

Cancer stem cells are capable of self-renewal, extensive proliferation, clonogenicity and resistance to treatment and are present in tumors with a worse prognosis (Reya et al. 2001). The coexposure condition increased stemness (increase in CD24+ and CD44+ markers and ALDH1A1/1A3). Moreover, high ALDH1A1/1A3 gene expression is associated with loss of hormonal receptors, poor survival, increased metastasis, angiogenesis and both were increased only in the

coexposure condition (Dieci et al. 2013). Among the hallmarks of metastasis specifically increased by the coexposure condition, anoikis, defined as the programmed cell death which occurs after detachment from the extra-cellular matrix was found. Certain cancer cells can develop resistance to anoikis through a complex mechanism, promoting invasiveness, resistance to treatment and metastasis (Adeshakin et al. 2021). Stemness and resistance to anoikis are closely linked and cancer stem cells can "protect" non cancer stem cells from anoikis (Kim et al. 2016). These hallmarks along with EMT, point towards resistance to chemotherapy. Cancer stem cells are thought to be able to escape the chemotherapy treatment (Reya et al. 2001). However, in contrast to other studies, we found no indicators of chemotherapy resistance in coculture condition (Lehuédé et al. 2019). Yet, the CSE seems to modify the mRNA expression of ABCG2 (increased in both CSE and coexposure conditions) and ABCC2 (increased by CSE).

Another interesting finding of our work is the presence of giant plurinuclear cells which can correspond to cell-in-cell structures, observed only in the coexposure condition. In a previous work on the effects of dioxin on breast cancer cells, similar structures were observed (Koual et al. 2021). These cell-in-cells can be the outcome of one cell engulfing the other (M et al. 2007). The prognostic value of this mechanism is uncertain. Here, the engulfing cell had a proliferative nucleus (Ki67 high) whereas the internalized cell was Ki67 negative. The cell in cell structures could be markers of poor prognosis through two mechanisms: i) the engulfed cell is providing nutrients to the "winner" cell and ii) the "winner" cell, involved in mitosis, will be blocked in an aneuploidy state which promotes tumor progression (Krishna and Overholtzer 2016); indeed, the eaten cell disrupts the division of "winner" cell by blocking mitosis, which can lead to cytokinesis failure and gross aneuploidy (Krishna and Overholtzer 2016). Since genomic instability is a hallmark of cancer, this could lead to breast cancer aggressiveness.

In cancer cells, EMT is also associated with poor prognosis (Kalluri and Weinberg 2009). The 3 main characteristics of EMT are loss of the epithelial phenotype, acquisition of mesenchymal properties and migration which were found only in the coexposure condition (Kalluri and Weinberg 2009). It must be noted that EMT is not a binary switch but a spectrum of minor modifications from epithelial to mesenchymal phenotype (Lüönd et al. 2021). *Vimentin*, *Fibronectin* and alpha-SMA were not modified in our work but are usually present at the later stage of EMT or "complete EMT" (Meyer-Schaller et al. 2019). Therefore, coculture and coexposure could promote a partial EMT, which is associated with metastasis (Lüönd et al. 2021). In partial EMT, the cells stay in a mesenchymal-epithelial plasticity state which makes it easier to reverse to the epithelial phenotype (MET) once in the metastatic organ. Indeed, Luong et al. found, in a mouse model of breast cancer, that cells with a complete EMT and a complete mesenchymal phenotype failed to colonized the lungs, whereas cells with a partial EMT succeeded (Lüönd et al. 2021).

Another marker of aggressiveness, the decrease of Er-α and PR, was found both in the coculture and coexposure conditions. Patients with tumors expressing those nuclear receptors can benefit from a specific treatment known as endocrine therapy, targeting these receptors which reduces their breast cancer recurrence rate by 50%, 15 years after the diagnosis (Early Breast Cancer Trialists' Collaborative Group (EBCTCG) 2005). However, 40-50% of women will develop an acquired resistance to their endocrine therapy in the first five years, altering severely their prognosis (Anurag et al. 2018). Moreover, a discordance in the expression of the hormonal receptors between the primary initial tumor and the metastatic recurrence is frequently found: up to 10 to 20% of patients had initially Er-α positive breast tumors with a Er-α negative metastatic recurrence (Yuda et al. 2019). To the best of our knowledge, this is the first study that evaluated the role of the environment in the loss of hormonal receptors.

Cigarette smoke extract increased the xenobiotic response pathways in the control and coculture condition. This pathway involved the AhR. We therefore hypothesized that the AhR, a xenobiotic receptor known to bind several compounds of the cigarette smoke such as benzo[a]pyrene, could mediate the aggressiveness promoted by the CSE in the coexposure condition, notably in endocrine resistance. Indeed, TCDD, an AhR agonist, also decreased Er-α and PR. Moreover, our work suggests that the effect of the CSE on cell migration could also be mediated by AhR. Indeed, cell migration was modified only in the coexposure condition after AhR KO. Pollutants present in the CSE could therefore lead to AhR activation explaining the migratory phenotype observed in the coexposure condition. Moreover, in AhR KO cells, both coculture and coexposure led to a similar increase in cell migration. This innovative finding suggests that the AhR signaling disruption could modify the interactions between the breast cells and pre-adipocytes. Further work must be carried out to confirm the role of the AhR.

Several limits to the present study must be noted. First, no *in vivo* validation of our results was carried out. Second, we studied only an acute exposure to CSE (48 hours) and not a chronic exposure. In the other study evaluating CSE on breast cancer aggressiveness, DiCello et al. exposed breast cancer cells and non-cancer cells to cigarette smoke extract or condensate for 40 or 72 weeks. They also found an increase in EMT, migration and tumorigenic properties (Di Cello et al. 2013). However, one main limit of their work is that they did not study breast cancer cells cocultured in their micro-environment. Our results suggest that an exposure of 48 hours is enough in a coculture *in vitro* model to highlight the deleterious effects of CSE. Finally, we chose to use a mixture of pollutants found in real life exposure, cigarette smoke. Little data exists on the exact composition of aqueous CSE. However, a recent study showed that more than 50 compounds were found in mainstream smoke of 1R6F Kentucky research

cigarettes (Jaccard et al. 2019). It is therefore difficult to know the exact role of each compound, especially since pollutants can interact with each other in many different ways (additive, synergistic, potentializing, antagonistic or dose dependent (Braun et al. 2016). Even though we are not able to determine with our work which pollutant is more the most critical driver of the mixture effect, this is the first time that a mixture of pollutants used in real like was found to promote breast cancer aggressiveness.

In conclusion, our work suggests that exposure to cigarette smoke could promote a more aggressive phenotype to breast cancer cells with a progression toward the implementation of metastasis (EMT, stemness, resistance to anoikis) and the resistance to therapy (notably endocrine therapy) when cocultured in conditions mimicking its micro-environnement. Even though several characteristics were assessed in triple negative MDA-MB-231 and HS-578T, we focused on ER+ MCF-7 cells, cells with the best prognosis and the best response to treatment. We hypothesized that this transformation could be mediated by the AhR. Our study emphasized the need to work with a coculture model since most of our results were seen in the coexposure condition (and not CSE only). Finally, this work, essential to public health, could help identify "at risk" patients of relapse and understand the mechanisms of breast cancer progression. This study also emphasizes the importance of promoting smoking cessation in breast cancer patients.

Data sharing: Data is available upon request.

Acknowledgements:

The authors acknowledge the cytometry core facility UMS cyto2BM, Université Paris Cité, for assistance with the generation of cytometry data. The authors also acknowledge the microscopy facility of Université Paris Cité for assistance.

The authors would like to thank Dr. David Sherr (Department of Environmental Health, Boston University School of Public Health, 72 East Concord St., Boston, MA 02118, USA) for providing cell lines, Dr. Franck Letourneur.and his team (GENOMI'C Platform, UDP-8104, University Paris Cité, Cochin institute, 75014 Paris) for the transcriptomic analysis and Dr. Sophie Lanone (IMRB, Mondor, France) for providing the research cigarettes.

Fundings: INSERM, Université Paris Cité, AP-HP, INCA TABAhR (n° TABAC18-037_AM)

Conflicts of interest: None

Author contributions:

Louise BENOIT: data curation, formal analysis, investigation, methodology, validation, visualisation, writing – original draft

Celine TOMKIEWICZ: conceptualisation, data curation, formal analysis, funding acquisition, investigation, methodology, project administration, resources, supervision, visualisation, writing– review & editing.

Maxime DELIT: data curation, formal analysis, investigation, methodology, writing– review & editing.

Hanna KHIDER: data curation, formal analysis, investigation, methodology, writing– review & editing.

Karine AUDOUZE: data curation, formal analysis, investigation, methodology, writing– review & editing.

Flavie KOWANDY: data curation, formal analysis, investigation, methodology, writing– review & editing.

Sylvie BORTOLI: data curation, formal analysis, investigation, methodology, writing– review & editing.

Robert BAROUKI: conceptualisation, formal analysis, funding acquisition, methodology, resources, supervision, validation, visualisation, writing– review & editing.

Xavier COUMOUL: conceptualisation, formal analysis, funding acquisition, methodology, resources, supervision, validation, visualisation, writing– original draft

Meriem KOUAL : conceptualisation, formal analysis, funding acquisition, methodology, resources, supervision, validation, visualisation, writing– review & editing.

References

Abraham BK, Fritz P, McClellan M, Hauptvogel P, Athelogou M, Brauch H. 2005. Prevalence of CD44+/CD24-/low cells in breast cancer may not be associated with clinical outcome but may favor distant metastasis. Clin Cancer Res Off J Am Assoc Cancer Res. 11(3):1154–1159.

Adeshakin FO, Adeshakin AO, Afolabi LO, Yan D, Zhang G, Wan X. 2021. Mechanisms for Modulating Anoikis Resistance in Cancer and the Relevance of Metabolic Reprogramming. Front Oncol. 11. [accessed 2022 Mar 3]. https://www.frontiersin.org/article/10.3389/fonc.2021.626577.

Althobiti M, El Ansari R, Aleskandarany M, Joseph C, Toss MS, Green AR, Rakha EA. 2020. The prognostic significance of ALDH1A1 expression in early invasive breast cancer. Histopathology. 77(3):437–448. doi:10.1111/his.14129.

Anurag M, Ellis MJ, Haricharan S. 2018. DNA damage repair defects as a new class of endocrine treatment resistance driver. Oncotarget. 9(91):36252–36253. doi:10.18632/oncotarget.26363.

Aubé M, Larochelle C, Ayotte P. 2011. Differential effects of a complex organochlorine mixture on the proliferation of breast cancer cell lines. Environ Res. 111(3):337–347. doi:10.1016/j.envres.2011.01.010.

Baskara I, Kerbrat S, Dagouassat M, Nguyen HQ, Guillot-Delost M, Surenaud M, Baillou C, Lemoine FM, Morin D, Boczkowski J, et al. 2020. Cigarette smoking induces human CCR6+Th17 lymphocytes senescence and VEGF-A secretion. Sci Rep. 10(1):6488. doi:10.1038/s41598-020-63613-4.

Benoit L, Jornod F, Zgheib E, Tomkiewicz C, Koual M, Coustillet T, Barouki R, Audouze K, Vinken M, Coumoul X. 2022. Adverse outcome pathway from activation of the AhR to breast cancer-related death. Environ Int. 165:107323. doi:10.1016/j.envint.2022.107323.

Blücher C, Stadler SC. 2017. Obesity and Breast Cancer: Current Insights on the Role of Fatty Acids and Lipid Metabolism in Promoting Breast Cancer Growth and Progression. Front Endocrinol. 8:293. doi:10.3389/fendo.2017.00293.

Borovski T, De Sousa E Melo F, Vermeulen L, Medema JP. 2011. Cancer stem cell niche: the place to be. Cancer Res. 71(3):634–639. doi:10.1158/0008-5472.CAN-10-3220.

Braun JM, Gennings C, Hauser R, Webster TF. 2016. What Can Epidemiological Studies Tell Us about the Impact of Chemical Mixtures on Human Health? Environ Health Perspect. 124(1):A6-9. doi:10.1289/ehp.1510569.

Bray F, Ferlay J, Soerjomataram I, Siegel RL, Torre LA, Jemal A. 2018. Global cancer statistics 2018: GLOBOCAN estimates of incidence and mortality worldwide for 36 cancers in 185 countries. CA Cancer J Clin. 68(6):394–424. doi:10.3322/caac.21492.

Ciccone V, Terzuoli E, Donnini S, Giachetti A, Morbidelli L, Ziche M. 2018. Stemness marker ALDH1A1 promotes tumor angiogenesis via retinoic acid/HIF-1α/VEGF signalling in MCF-7 breast cancer cells. J Exp Clin Cancer Res. 37(1):311. doi:10.1186/s13046-018-0975-0.

Cooper JA, Rohan TE, Cant EL, Horsfall DJ, Tilley WD. 1989. Risk factors for breast cancer by oestrogen receptor status: a population-based case-control study. Br J Cancer. 59(1):119–125. doi:10.1038/bjc.1989.24.

Croker AK, Rodriguez-Torres M, Xia Y, Pardhan S, Leong HS, Lewis JD, Allan AL. 2017. Differential Functional Roles of ALDH1A1 and ALDH1A3 in Mediating Metastatic Behavior and Therapy Resistance of Human Breast Cancer Cells. Int J Mol Sci. 18(10):2039. doi:10.3390/ijms18102039.

Di Cello F, Flowers VL, Li H, Vecchio-Pagán B, Gordon B, Harbom K, Shin J, Beaty R, Wang W, Brayton C, et al. 2013. Cigarette smoke induces epithelial to mesenchymal transition and increases the metastatic ability of breast cancer cells. Mol Cancer. 12:90. doi:10.1186/1476-4598-12-90.

Dieci MV, Barbieri E, Piacentini F, Ficarra G, Bettelli S, Dominici M, Conte PF, Guarneri V. 2013. Discordance in receptor status between primary and recurrent breast cancer has a prognostic impact: a single-institution analysis. Ann Oncol Off J Eur Soc Med Oncol. 24(1):101–108. doi:10.1093/annonc/mds248.

Early Breast Cancer Trialists' Collaborative Group (EBCTCG). 2005. Effects of chemotherapy and hormonal therapy for early breast cancer on recurrence and 15-year survival: an overview of the randomised trials. Lancet Lond Engl. 365(9472):1687–1717. doi:10.1016/S0140-6736(05)66544-0.

Ginestier C, Hur MH, Charafe-Jauffret E, Monville F, Dutcher J, Brown M, Jacquemier J, Viens P, Kleer CG, Liu S, et al. 2007. ALDH1 is a marker of normal and malignant human mammary stem cells and a predictor of poor clinical outcome. Cell Stem Cell. 1(5):555–567. doi:10.1016/j.stem.2007.08.014.

Jaccard G, Djoko DT, Korneliou A, Stabbert R, Belushkin M, Esposito M. 2019. Mainstream smoke constituents and in vitro toxicity comparative analysis of 3R4F and 1R6F reference cigarettes. Toxicol Rep. 6:222–231. doi:10.1016/j.toxrep.2019.02.009.

Joussaume A, Karayan-Tapon L, Benzakour O, Dkhissi F. 2020. A Comparative Study of Anoikis Resistance Assays for Tumor Cells. Biomed J Sci Tech Res. 29(2):22255–22262. doi:10.26717/BJSTR.2020.29.004767.

Kalluri R, Weinberg RA. 2009. The basics of epithelial-mesenchymal transition. J Clin Invest. 119(6):1420–1428. doi:10.1172/JCI39104.

Khoury T, Ademuyiwa FO, Chandraseekhar R, Jabbour M, DeLeo A, Ferrone S, Wang Y, Wang X. 2012. Aldehyde dehydrogenase 1A1 expression in breast cancer is associated with stage, triple negativity, and outcome to neoadjuvant chemotherapy. Mod Pathol. 25(3):388–397. doi:10.1038/modpathol.2011.172.

Kim MJ, Pelloux V, Guyot E, Tordjman J, Bui L-C, Chevallier A, Forest C, Benelli C, Clément K, Barouki R. 2012. Inflammatory pathway genes belong to major targets of persistent organic pollutants in adipose cells. Environ Health Perspect. 120(4):508–514. doi:10.1289/ehp.1104282.

Kim S-Y, Hong S-H, Basse PH, Wu C, Bartlett DL, Kwon YT, Lee YJ. 2016. Cancer Stem Cells Protect Non-Stem Cells From Anoikis: Bystander Effects. J Cell Biochem. 117(10):2289–2301. doi:10.1002/jcb.25527.

Kothari C, Diorio C, Durocher F. 2020. The Importance of Breast Adipose Tissue in Breast Cancer. Int J Mol Sci. 21(16):5760. doi:10.3390/ijms21165760.

Koual M, Tomkiewicz C, Guerrera IC, Sherr D, Barouki R, Coumoul X. 2021. Aggressiveness and Metastatic Potential of Breast Cancer Cells Co-Cultured with Preadipocytes and Exposed to an Environmental Pollutant Dioxin: An in Vitro and in Vivo Zebrafish Study. Environ Health Perspect. 129(3):37002. doi:10.1289/EHP7102.

Krishna S, Overholtzer M. 2016. Mechanisms and consequences of entosis. Cell Mol Life Sci CMLS. 73(11–12):2379–2386. doi:10.1007/s00018-016-2207-0.

Lee Y, Jung WH, Koo JS. 2015. Adipocytes can induce epithelial-mesenchymal transition in breast cancer cells. Breast Cancer Res Treat. 153(2):323–335. doi:10.1007/s10549-015-3550-9.

Lehuédé C, Li X, Dauvillier S, Vaysse C, Franchet C, Clement E, Esteve D, Longué M, Chaltiel L, Le Gonidec S, et al. 2019. Adipocytes promote breast cancer resistance to chemotherapy, a process amplified by obesity: role of the major vault protein (MVP). Breast Cancer Res BCR. 21(1):7. doi:10.1186/s13058-018-1088-6.

Li W, Ma H, Zhang J, Zhu L, Wang C, Yang Y. 2017. Unraveling the roles of CD44/CD24 and ALDH1 as cancer stem cell markers in tumorigenesis and metastasis. Sci Rep. 7(1):13856. doi:10.1038/s41598-017-14364-2.

Lin P-H, Lin C-H, Huang C-C, Chuang M-C, Lin P. 2007. 2,3,7,8-Tetrachlorodibenzo-p-dioxin (TCDD) induces oxidative stress, DNA strand breaks, and poly(ADP-ribose) polymerase-1 activation in human breast carcinoma cell lines. Toxicol Lett. 172(3):146–158. doi:10.1016/j.toxlet.2007.06.003.

Lin P-H, Lin C-H, Huang C-C, Fang J-P, Chuang M-C. 2008. 2,3,7,8-Tetrachlorodibenzo-p-dioxin modulates the induction of DNA strand breaks and poly(ADP-ribose) polymerase-1 activation by 17beta-estradiol in human breast carcinoma cells through alteration of CYP1A1 and CYP1B1 expression. Chem Res Toxicol. 21(7):1337–1347. doi:10.1021/tx700396d.

Lüönd F, Sugiyama N, Bill R, Bornes L, Hager C, Tang F, Santacroce N, Beisel C, Ivanek R, Bürglin T, et al. 2021. Distinct contributions of partial and full EMT to breast cancer malignancy. Dev Cell. 56(23):3203-3221.e11. doi:10.1016/j.devcel.2021.11.006.

M O, Aa M, G M, G N, Sj S, Rw K, Es C, Js B. 2007. A nonapoptotic cell death process, entosis, that occurs by cell-in-cell invasion. Cell. 131(5). doi:10.1016/j.cell.2007.10.040. [accessed 2022 Mar 1]. https://pubmed.ncbi.nlm.nih.gov/18045538/.

Manjer J, Malina J, Berglund G, Bondeson L, Garne JP, Janzon L. 2001. Smoking associated with hormone receptor negative breast cancer. Int J Cancer. 91(4):580–584. doi:10.1002/1097-0215(200002)9999:9999<::aid-ijc1091>3.0.co;2-v.

Meyer-Schaller N, Cardner M, Diepenbruck M, Saxena M, Tiede S, Lüönd F, Ivanek R, Beerenwinkel N, Christofori G. 2019. A Hierarchical Regulatory Landscape during the Multiple Stages of EMT. Dev Cell. 48(4):539-553.e6. doi:10.1016/j.devcel.2018.12.023.

Miret N, Pontillo C, Ventura C, Carozzo A, Chiappini F, Kleiman de Pisarev D, Fernández N, Cocca C, Randi A. 2016. Hexachlorobenzene modulates the crosstalk between the aryl hydrocarbon receptor and transforming growth factor-β1 signaling, enhancing human breast cancer cell migration and invasion. Toxicology. 366–367:20–31. doi:10.1016/j.tox.2016.08.007.

Murin S, Inciardi J. 2001. Cigarette smoking and the risk of pulmonary metastasis from breast cancer. Chest. 119(6):1635–1640. doi:10.1378/chest.119.6.1635.

Narasimhan S, Stanford Zulick E, Novikov O, Parks AJ, Schlezinger JJ, Wang Z, Laroche F, Feng H, Mulas F, Monti S, et al. 2018. Towards Resolving the Pro- and Anti-Tumor Effects of the Aryl Hydrocarbon Receptor. Int J Mol Sci. 19(5):1388. doi:10.3390/ijms19051388.

Nechuta S, Chen WY, Cai H, Poole EM, Kwan ML, Flatt SW, Patterson RE, Pierce JP, Caan BJ, Ou Shu X. 2016. A pooled analysis of post-diagnosis lifestyle factors in association with late estrogen-receptor-positive breast cancer prognosis. Int J Cancer. 138(9):2088–2097. doi:10.1002/ijc.29940.

Paget S. 1989. The distribution of secondary growths in cancer of the breast. 1889. Cancer Metastasis Rev. 8(2):98–101.

Paoli P, Giannoni E, Chiarugi P. 2013. Anoikis molecular pathways and its role in cancer progression. Biochim Biophys Acta. 1833(12):3481–3498. doi:10.1016/j.bbamcr.2013.06.026.

Pierce JP, Patterson RE, Senger CM, Flatt SW, Caan BJ, Natarajan L, Nechuta SJ, Poole EM, Shu X-O, Chen WY. 2014. Lifetime cigarette smoking and breast cancer prognosis in the After Breast Cancer Pooling Project. J Natl Cancer Inst. 106(1):djt359. doi:10.1093/jnci/djt359.

Pontillo C, Español A, Chiappini F, Miret N, Cocca C, Alvarez L, Kleiman de Pisarev D, Sales ME, Randi AS. 2015. Hexachlorobenzene promotes angiogenesis in vivo, in a breast cancer model and neovasculogenesis in vitro, in the human microvascular endothelial cell line HMEC-1. Toxicol Lett. 239(1):53–64. doi:10.1016/j.toxlet.2015.09.001.

Pontillo CA, Rojas P, Chiappini F, Sequeira G, Cocca C, Crocci M, Colombo L, Lanari C, Kleiman de Pisarev D, Randi A. 2013. Action of hexachlorobenzene on tumor growth and metastasis in different experimental models. Toxicol Appl Pharmacol. 268(3):331–342. doi:10.1016/j.taap.2013.02.007.

Rajapakse N, Silva E, Kortenkamp A. 2002. Combining xenoestrogens at levels below individual no-observed-effect concentrations dramatically enhances steroid hormone action. Environ Health Perspect. 110(9):917–921. doi:10.1289/ehp.02110917.

Reya T, Morrison SJ, Clarke MF, Weissman IL. 2001. Stem cells, cancer, and cancer stem cells. Nature. 414(6859):105–111. doi:10.1038/35102167.

Rodriguez A-M, Elabd C, Amri E-Z, Ailhaud G, Dani C. 2005. The human adipose tissue is a source of multipotent stem cells. Biochimie. 87(1):125–128. doi:10.1016/j.biochi.2004.11.007.

Rybinska I, Agresti R, Trapani A, Tagliabue E, Triulzi T. 2020. Adipocytes in Breast Cancer, the Thick and the Thin. Cells. 9(3):560. doi:10.3390/cells9030560.

Schneider CA, Rasband WS, Eliceiri KW. 2012. NIH Image to ImageJ: 25 years of image analysis. Nat Methods. 9(7):671–675. doi:10.1038/nmeth.2089.

Siegel RL, Miller KD, Fuchs HE, Jemal A. 2021. Cancer Statistics, 2021. CA Cancer J Clin. 71(1):7–33. doi:10.3322/caac.21654.

Silva E, Rajapakse N, Kortenkamp A. 2002. Something from "nothing"--eight weak estrogenic chemicals combined at concentrations below NOECs produce significant mixture effects. Environ Sci Technol. 36(8):1751–1756. doi:10.1021/es0101227.

Sjöström M, Hartman L, Honeth G, Grabau D, Malmström P, Hegardt C, Fernö M, Niméus E. 2015. Stem cell biomarker ALDH1A1 in breast cancer shows an association with prognosis and clinicopathological variables that is highly cut-off dependent. J Clin Pathol. 68(12):1012–1019. doi:10.1136/jclinpath-2015-203092.

Stanford EA, Wang Z, Novikov O, Mulas F, Landesman-Bollag E, Monti S, Smith BW, Seldin DC, Murphy GJ, Sherr DH. 2016. The role of the aryl hydrocarbon receptor in the development of cells with the molecular and functional characteristics of cancer stem-like cells. BMC Biol. 14:20. doi:10.1186/s12915-016-0240-y.

Yuda S, Shimizu C, Yoshida M, Shiino S, Kinoshita T, Maeshima AM, Tamura K. 2019. Biomarker discordance between primary breast cancer and bone or bone marrow metastases. Jpn J Clin Oncol. 49(5):426–430. doi:10.1093/jjco/hyz018.

Zárate LV, Pontillo CA, Español A, Miret NV, Chiappini F, Cocca C, Álvarez L, de Pisarev DK, Sales ME, Randi AS. 2020. Angiogenesis signaling in breast cancer models is induced by hexachlorobenzene and chlorpyrifos, pesticide ligands of the aryl hydrocarbon receptor. Toxicol Appl Pharmacol. 401:115093. doi:10.1016/j.taap.2020.115093.

Figure legends

Figure 1. Study protocol

Breast cancer cells lines, MCF-7 or MDA-MB-231 were plated in a 6 well plate with 400 000 cells per well with or without coculture (200 000 hMADS). After 24 hours, they were treated by CSE 1% for 48 hours. The cells were then analyzed and a comparison between control (MCF-7 cells, alone), CSE (MCF-7 cells treated with 1%CSE), coculture (MCF-7 cocultured with hMADS), and coexposure (coculture with CSE) was carried out

Figure 2. Morphological differences of MCF-7 cells between control cells, treatment by cigarette smoke extract (CSE), coculture (hMADS) or coexposure (hMADS + CSE).

A. After 48 hours of treatment, the cells were then fixed and stained for paxillin (red), actin (green), and nucleus (blue). Scale bar 20 um. Symbols were used to point out the lamellipods (arrow), cells in cells (*) and giant cells (#)
B. To explore the giant cell in cell structures, the cells were fixed and stained for actin (red), Ki67 (green), and nucleus (blue). Scale bar 20 um. Symbols were used to point out the cells in cells (arrow) structures. The internalized cell is KI67 negative and thus in a state of quiescence, while the host cell is KI67 positive.
C. The cells were fixed and stained and stained for E-cadherin (green) and nucleus (blue). Scale bar 10 um. Symbols were used to point out the internalization of the E-cadherin and the loss of the cell-cell junction (arrow) and cells in cells (*).

Figure 3. Comparison of cell migration between control cells, treatment by cigarette smoke extract (CSE), coculture (hMADS) or coexposure (hMADS + CSE)

A. *MCF-7 cells (N=4)*: After 48 hours of treatment, the cells were plated in a Boyden chamber with a gradient of serum (upper chamber without serum and 10% serum in the lower chamber). Cell migration was assessed with Hoechst staining and photographed using a PICO device. The number of migrated cells was compared between the conditions. The numerical mean +/- SEM are represented and a (Kruskal–Wallis's H test (nonparametric comparison of k independent series) followed by a 1-factor ANOVA test (parametric comparison of k independent series) were carried out (* $p<0.05$).

B. *HS-578 Cas 9 and HS-578T AhR KO cells*: Migration was evaluated using xCELLigence dynamic monitoring. The evolution of the cell index for each condition was determined by analyzing the slope of the line in the interval [0- 20 h]. The graph represents the mean slope compared to the control ± SEM for 5 measurements. A representative graph from xCELLigence system is presented in Figure SX. The numerical mean +/- SEM are represented and a Kruskal–Wallis's H test (nonparametric comparison of k independent series) followed by a 1-factor ANOVA test (parametric comparison of k independent series) were carried out (* $p<0.05$, ** $p<0.01$).

Figure 4. Semi-quantification and comparison of epithelial to mesenchymal transition using qPCR for MCF-7 cells between control cells, treatment by cigarette smoke extract (CSE), coculture (hMADS) or coexposure (hMADS + CSE)

A qPCR was then performed with genes involved in epithelial to mesenchymal transition (n=7) and compared between conditions using a Kruskal–Wallis's H test (nonparametric comparison of k independent series) followed by a 1-factor ANOVA test (parametric comparison of k independent series) (* $p<0.05$ **, $p<0.01$, *** $p<0.001$ et **** $p<0.0001$).

Figure 5. Comparison of stemness using a qPCR and cell cytometry for MCF-7 cells between control cells, treatment by cigarette smoke extract (CSE), coculture (hMADS) or coexposure (hMADS + CSE)

A. *Cytometry assay CD24/CD44 (n=4):* The cells were marked by BV421-CD44 and FITC-CD24 and analyzed by flow cytometry. The number of CD 24 high and CD 44 high cells are presented as percentages compared to the control condition. The detail can be found in Supplementary Figure S6.
B. *Semi-quantification of genes involved in stemness:* A qPCR was performed with genes involved in stemness (ALDH1A1, n=7 and ALDH1A3, n=10). Conditions were compared using a Kruskal–Wallis's H test (nonparametric comparison of k independent series) followed by a 1-factor ANOVA test (parametric comparison of k independent series) (* $p<0.05$ **, $p<0.01$, *** $p<0.001$ et **** $p<0.0001$).

Figure 6. Comparison of anchorage independents growth for MCF-7 cells between control cells, treatment by cigarette smoke extract (CSE), coculture (hMADS) or coexposure (hMADS + CSE) (N=4)

After treatment, the cells were plated in a 24 well plate in an agar gradient (base agar 0,6% and top agar 0,4).The number and size of colonies were compared after 28 days The wells were photographed (Scale bar 100 µm) (A) and the colony size and number was compared between the conditions (B and C) using a Kruskal–Wallis's H test (nonparametric comparison of k independent series) followed by a 1-factor ANOVA test (parametric comparison of k independent series) (*** $p<0.001$, **** $p<0.0001$).

Figure 7. Comparison of hormonal receptors for MCF-7 cells between control cells, treatment by cigarette smoke extract (CSE), coculture (hMADS) or coexposure (hMADS + CSE) and evaluation of the role of an AhR agonist (TCDD)

A. *MCF-7 cells:* RNA semi-quantification of *Er-α* (n=10), *ER-β* (N=6) and *PR* (n=7) were carried out by qPCR:.* $p<0.05$ **, $p<0.01$, *** $p<0.001$ et **** $p<0.0001$
B. *MCF-7 cells:* Protein quantification was carried out for Er-α (long isoform, 66kDA) (n=3) and were normalized to actin level and non-treated condition: .* $p<0.05$ **, $p<0.01$, *** $p<0.001$ et **** $p<0.0001$
C. *Role of an AhR agonist (TCDD):* RNA semi-quantification of *Er-α* (n=6) and *Er-β* (N=6) were carried out by qPCR:.* $p<0.05$ **, $p<0.01$, *** $p<0.001$ and **** $p<0.0001$
D. *Role of an AhR agonist (TCDD):* Protein quantification was carried out for Er-α (long isoform, 66kDA) and were normalized to actin level and non-treated condition (n=7) : * $p<0.05$ **, $p<0.01$, *** $p<0.001$ and **** $p<0.0001$

Figure 8. Transcriptomic analysis of MCF-7 cells according to the different conditions: control cells, treatment by cigarette smoke extract (CSE), coculture (hMADS) or coexposure (hMADS + CSE)

A. After RNA sequencing, a differential analysis was carried out using DESeq2 package from the R softwareShinyGo v0.75 Gene Ontology Enrichment Analysis software was used for the analysis of the signaling pathways involved using the Kyoto Encyclopedia of Genes and Genomes (KEGG) database.
B. Pathways upregulated and downregulated are presented.

C. Differential analysis of genes specifically modified by CSE in coculture or without. Venn diagram representing specific pathways to CSE without or with coculture and common pathways of CSE in both conditions (Fold >1.5 or <0.75, $p<0.05$, top 30 terms) using the KEGG database on ShinyGo v0.75.

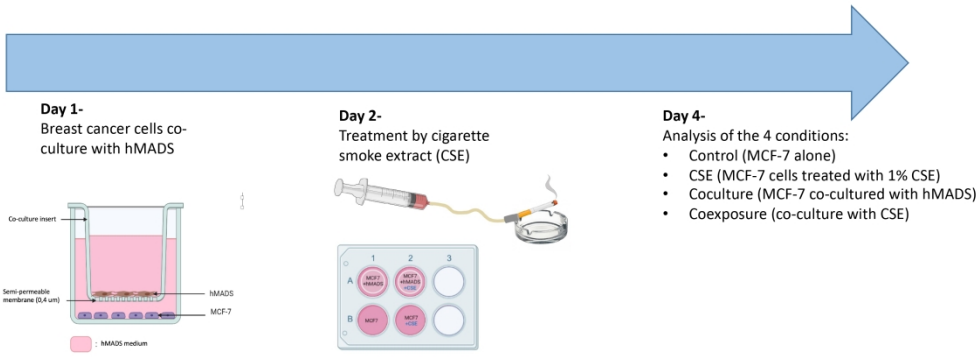

Figure 1. Study protocol

Breast cancer cells lines, MCF-7 or MDA-MB-231 were plated in a 6 well plate with 400 000 cells per well with or without coculture (200 000 hMADS). After 24 hours, they were treated by CSE 1% for 48 hours. The cells were then analyzed and a comparison between control (MCF-7 cells, alone), CSE (MCF-7 cells treated with 1%CSE), coculture (MCF-7 cocultured with hMADS), and coexposure (coculture with CSE) was carried out

302x112mm (300 x 300 DPI)

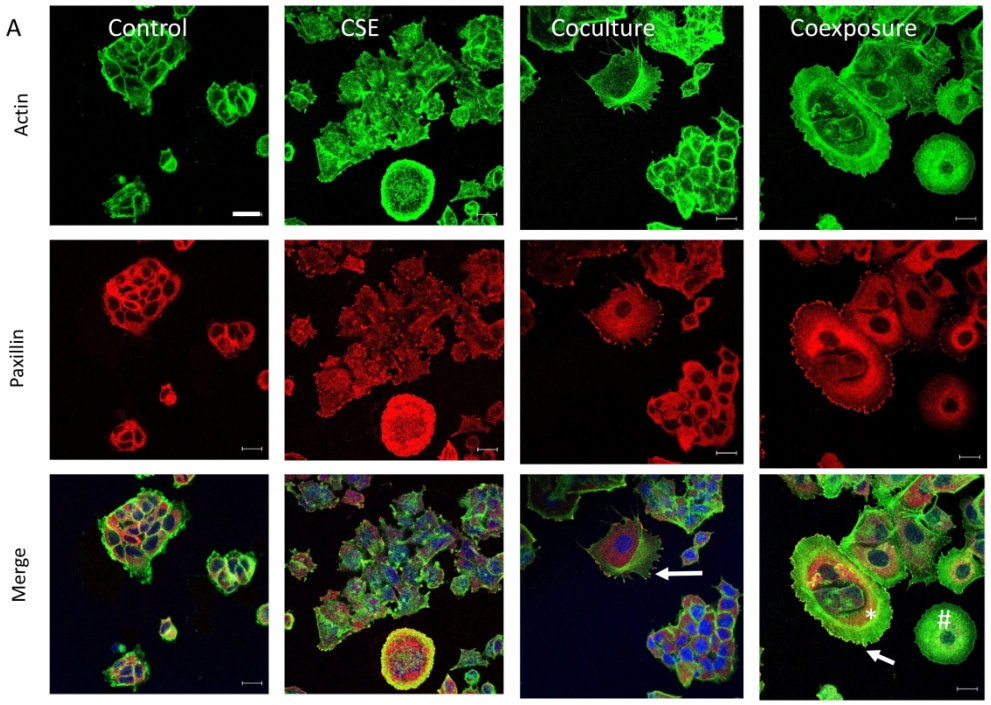

Figure 2A. Morphological differences of MCF-7 cells between control cells, treatment by cigarette smoke extract (CSE), coculture (hMADS) or coexposure (hMADS + CSE).
A. After 48 hours of treatment, the cells were then fixed and stained for paxillin (red), actin (green), and nucleus (blue). Scale bar 20 um. Symbols were used to point out the lamellipods (arrow), cells in cells (*) and giant cells (#)

238x171mm (300 x 300 DPI)

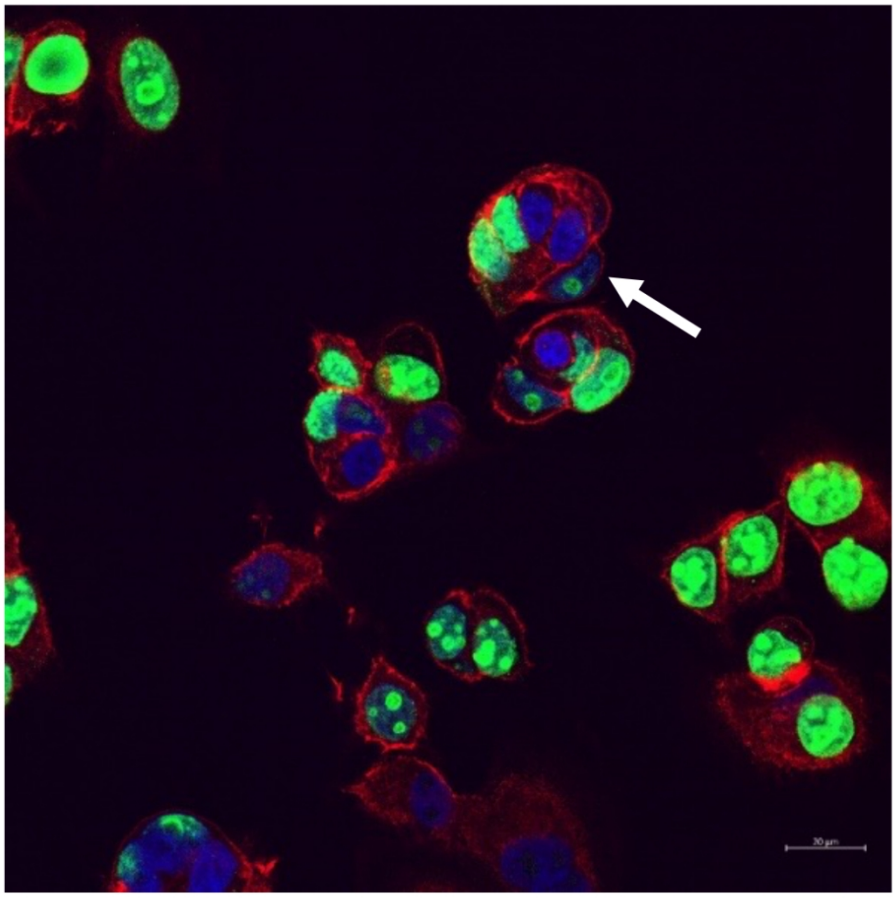

Figure 2B. Morphological differences of MCF-7 cells between control cells, treatment by cigarette smoke extract (CSE), coculture (hMADS) or coexposure (hMADS + CSE).
B. To explore the giant cell in cell structures, the cells were fixed and stained for actin (red), Ki67 (green), and nucleus (blue). Scale bar 20 um. Symbols were used to point out the cells in cells (arrow) structures. The internalized cell is KI67 negative and thus in a state of quiescence, while the host cell is KI67 positive.

98x93mm (300 x 300 DPI)

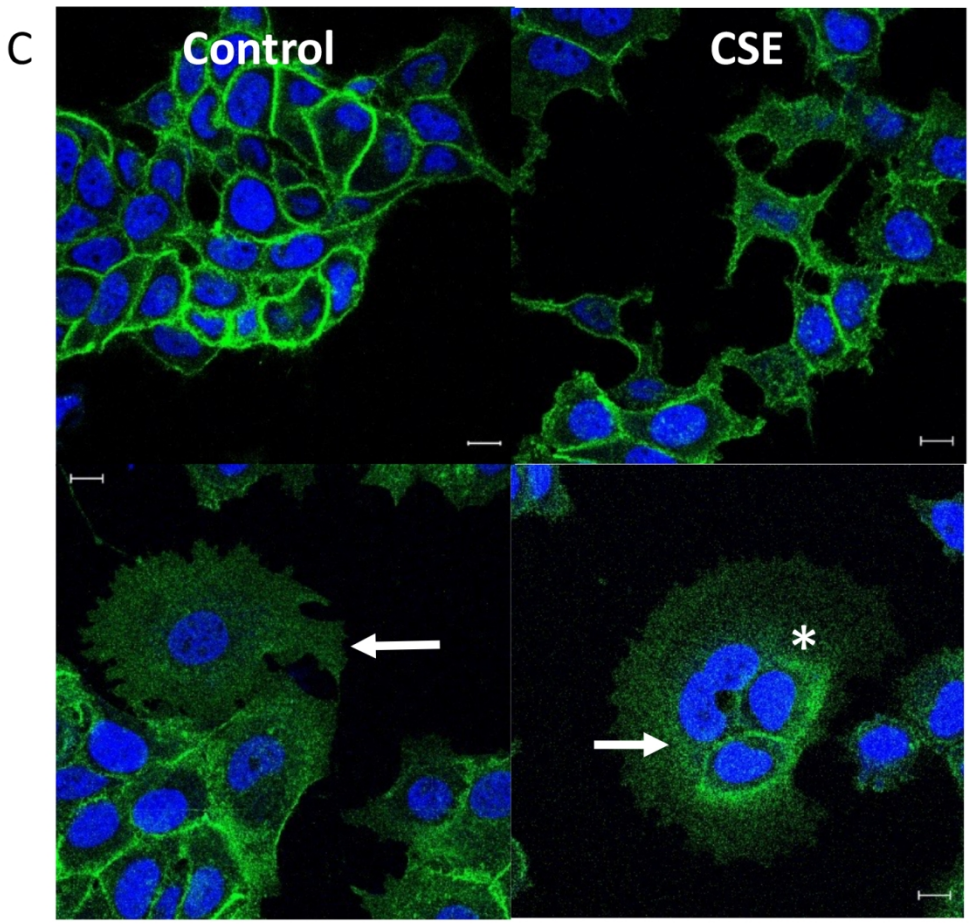

Figure 2C. Morphological differences of MCF-7 cells between control cells, treatment by cigarette smoke extract (CSE), coculture (hMADS) or coexposure (hMADS + CSE).
C. The cells were fixed and stained and stained for E-cadherin (green) and nucleus (blue). Scale bar 10 um. Symbols were used to point out the internalization of the E-cadherin and the loss of the cell-cell junction (arrow) and cells in cells (*).

126x121mm (300 x 300 DPI)

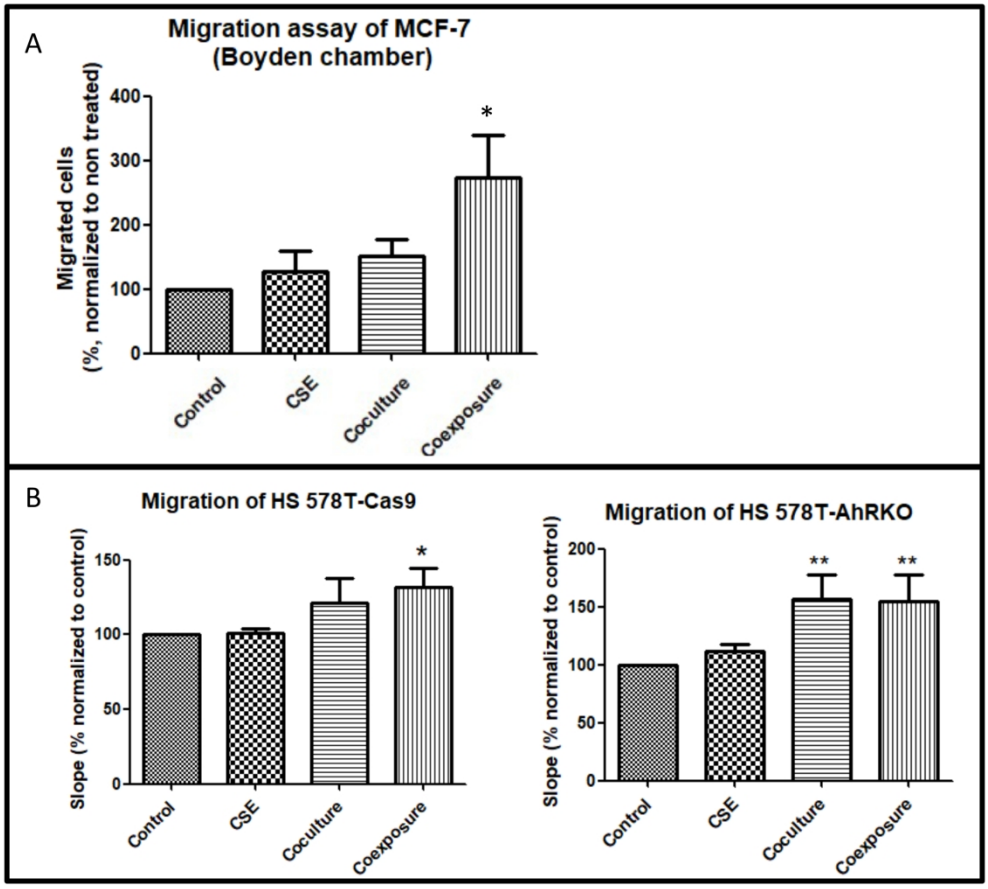

Figure 3. Comparison of cell migration between control cells, treatment by cigarette smoke extract (CSE), coculture (hMADS) or coexposure (hMADS + CSE)

A. MCF-7 cells (N=4): After 48 hours of treatment, the cells were plated in a Boyden chamber with a gradient of serum (upper chamber without serum and 10% serum in the lower chamber). Cell migration was assessed with Hoechst staining and photographed using a PICO device. The number of migrated cells was compared between the conditions. The numerical mean +/- SEM are represented and a (Kruskal–Wallis's H test (nonparametric comparison of k independent series) followed by a 1-factor ANOVA test (parametric comparison of k independent series) were carried out (* $p<0.05$).

B. HS-578 Cas 9 and HS-578T AhR KO cells: Migration was evaluated using xCELLigence dynamic monitoring. The evolution of the cell index for each condition was determined by analyzing the slope of the line in the interval [0- 20 h]. The graph represents the mean slope compared to the control ± SEM for 5 measurements. A representative graph from xCELLigence system is presented in Figure SX. The numerical mean +/- SEM are represented and a Kruskal–Wallis's H test (nonparametric comparison of k independent series) followed by a 1-factor ANOVA test (parametric comparison of k independent series) were carried out (* $p<0.05$, ** $p<0.01$).

Figure 3. Comparison of cell migration between control cells, treatment by cigarette smoke extract (CSE), coculture (hMADS) or coexposure (hMADS + CSE)

A. MCF-7 cells (N=4): After 48 hours of treatment, the cells were plated in a Boyden chamber with a gradient of serum (upper chamber without serum and 10% serum in the lower chamber). Cell migration was assessed with Hoechst staining and photographed using a PICO device. The number of migrated cells was compared between the conditions. The numerical mean +/- SEM are represented and a (Kruskal–Wallis's H test (nonparametric comparison of k independent series) followed by a 1-factor ANOVA test (parametric comparison of k independent series) were carried out (* $p<0.05$).

B. HS-578 Cas 9 and HS-578T AhR KO cells: Migration was evaluated using xCELLigence dynamic monitoring. The evolution of the cell index for each condition was determined by analyzing the slope of the line in the interval [0- 20 h]. The graph represents the mean slope compared to the control ± SEM for 5 measurements. A representative graph from xCELLigence system is presented in Figure SX. The numerical mean +/- SEM are represented and a Kruskal–Wallis's H test (nonparametric comparison of k independent series) followed by a 1-factor ANOVA test (parametric comparison of k independent series) were carried out (* $p<0.05$, ** $p<0.01$).

206x185mm (300 x 300 DPI)

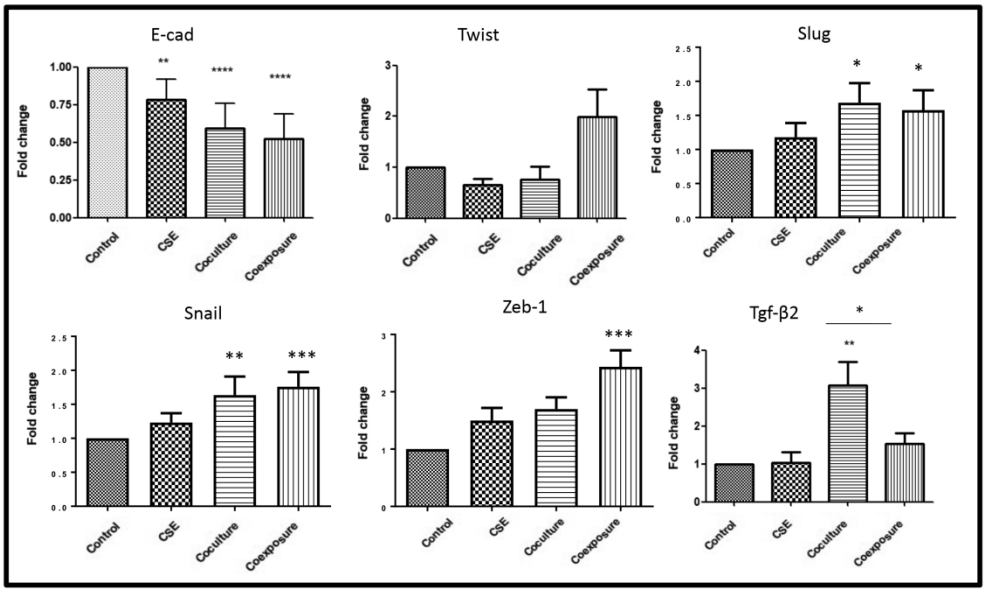

Figure 4. Semi-quantification and comparison of epithelial to mesenchymal transition using qPCR for MCF-7 cells between control cells, treatment by cigarette smoke extract (CSE), coculture (hMADS) or coexposure (hMADS + CSE)

A qPCR was then performed with genes involved in epithelial to mesenchymal transition (n=7) and compared between conditions using a Kruskal–Wallis's H test (nonparametric comparison of k independent series) followed by a 1-factor ANOVA test (parametric comparison of k independent series) (* $p<0.05$ **, $p<0.01$, *** $p<0.001$ et **** $p<0.0001$).

Figure 4. Semi-quantification and comparison of epithelial to mesenchymal transition using qPCR for MCF-7 cells between control cells, treatment by cigarette smoke extract (CSE), coculture (hMADS) or coexposure (hMADS + CSE)

A qPCR was then performed with genes involved in epithelial to mesenchymal transition (n=7) and compared between conditions using a Kruskal–Wallis's H test (nonparametric comparison of k independent series) followed by a 1-factor ANOVA test (parametric comparison of k independent series) (* $p<0.05$ **, $p<0.01$, *** $p<0.001$ et **** $p<0.0001$).

213x128mm (300 x 300 DPI)

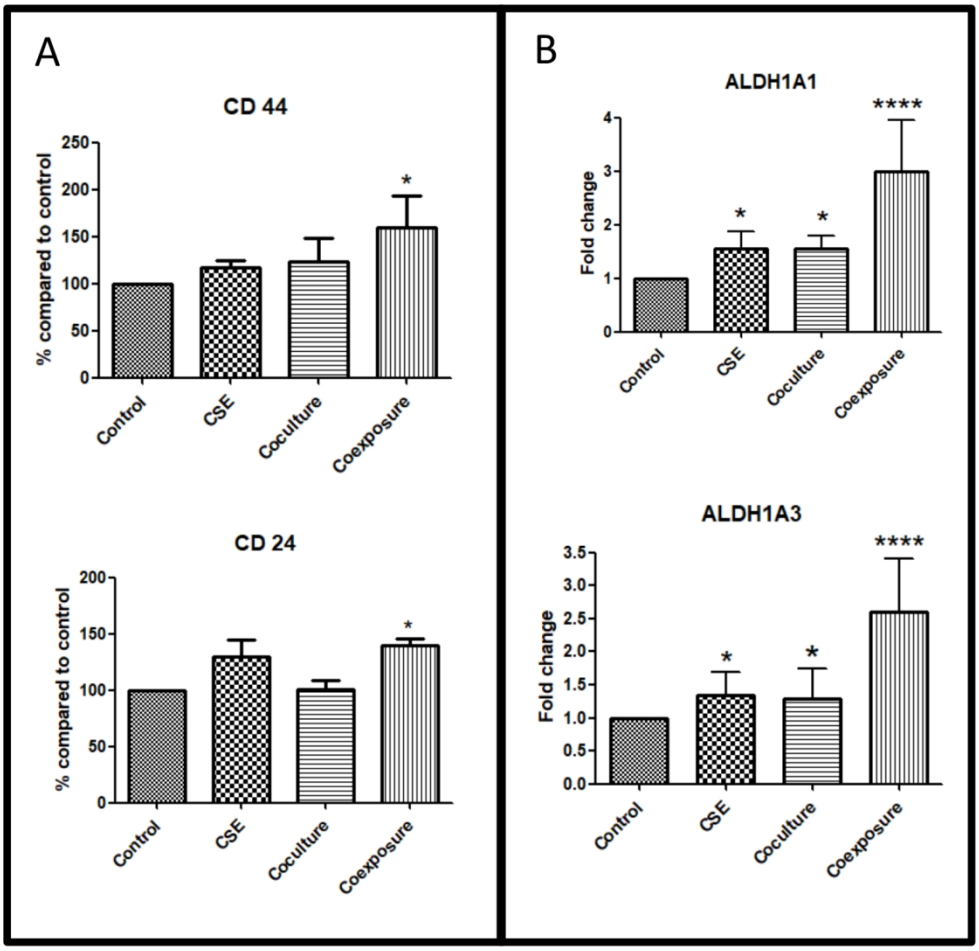

Figure 5. Comparison of stemness using a qPCR and cell cytometry for MCF-7 cells between control cells, treatment by cigarette smoke extract (CSE), coculture (hMADS) or coexposure (hMADS + CSE)
A. Cytometry assay CD24/CD44 (n=4): The cells were marked by BV421-CD44 and FITC-CD24 and analyzed by flow cytometry. The number of CD 24 high and CD 44 high cells are presented as percentages compared to the control condition. The detail can be found in Supplementary Figure S6.
B. Semi-quantification of genes involved in stemness: A qPCR was performed with genes involved in stemness (ALDH1A1, n=7 and ALDH1A3, n=10). Conditions were compared using a Kruskal–Wallis's H test (nonparametric comparison of k independent series) followed by a 1-factor ANOVA test (parametric comparison of k independent series) (* $p<0.05$ **, $p<0.01$, *** $p<0.001$ et **** $p<0.0001$).

140x136mm (300 x 300 DPI)

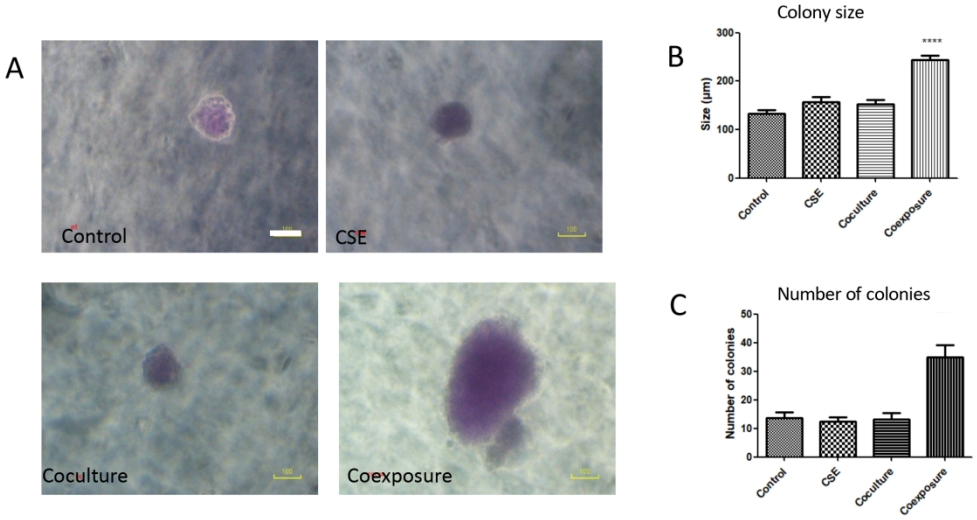

Figure 6. Comparison of anchorage independents growth for MCF-7 cells between control cells, treatment by cigarette smoke extract (CSE), coculture (hMADS) or coexposure (hMADS + CSE) (N=4)
After treatment, the cells were plated in a 24 well plate in an agar gradient (base agar 0,6% and top agar 0,4).The number and size of colonies were compared after 28 days The wells were photographed (Scale bar 100 µm) (A) and the colony size and number was compared between the conditions (B and C) using a Kruskal–Wallis's H test (nonparametric comparison of k independent series) followed by a 1-factor ANOVA test (parametric comparison of k independent series) (*** p<0.001, **** p<0.0001).

Figure 6. Comparison of anchorage independents growth for MCF-7 cells between control cells, treatment by cigarette smoke extract (CSE), coculture (hMADS) or coexposure (hMADS + CSE) (N=4)
After treatment, the cells were plated in a 24 well plate in an agar gradient (base agar 0,6% and top agar 0,4).The number and size of colonies were compared after 28 days The wells were photographed (Scale bar 100 µm) (A) and the colony size and number was compared between the conditions (B and C) using a Kruskal–Wallis's H test (nonparametric comparison of k independent series) followed by a 1-factor ANOVA test (parametric comparison of k independent series) (*** p<0.001, **** p<0.0001).

192x103mm (300 x 300 DPI)

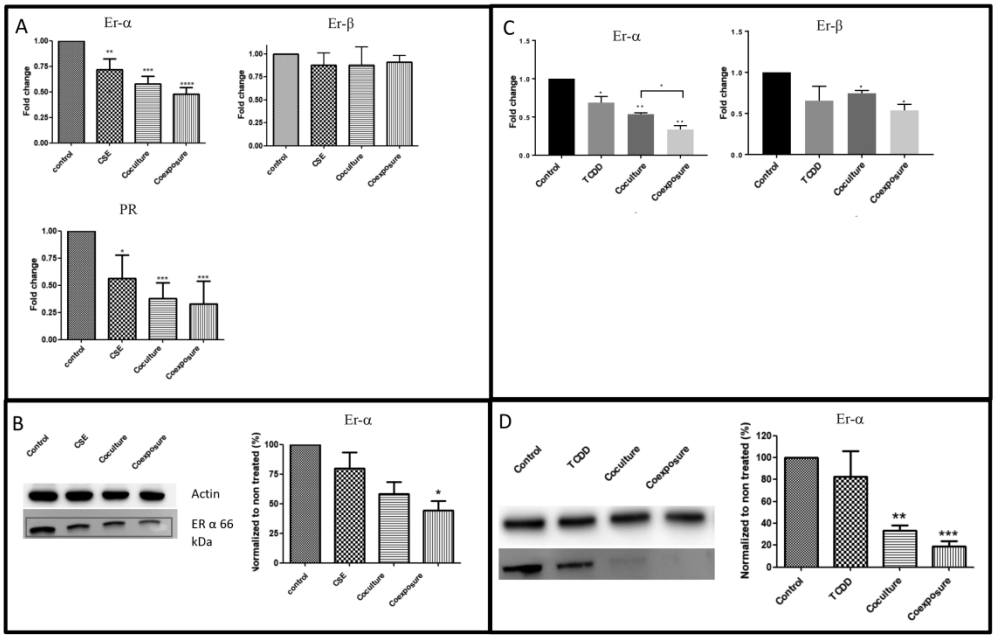

Figure 7. Comparison of hormonal receptors for MCF-7 cells between control cells, treatment by cigarette smoke extract (CSE), coculture (hMADS) or coexposure (hMADS + CSE) and evaluation of the role of an AhR agonist (TCDD)

A. MCF-7 cells: RNA semi-quantification of Er-α (n=10), ER-β (N=6) and PR (n=7) were carried out by qPCR:.* $p<0.05$ **, $p<0.01$, *** $p<0.001$ et **** $p<0.0001$

B. MCF-7 cells: Protein quantification was carried out for Er-α (long isoform, 66kDA) (n=3) and were normalized to actin level and non-treated condition: .* $p<0.05$ **, $p<0.01$, *** $p<0.001$ et **** $p<0.0001$

C. Role of an AhR agonist (TCDD): RNA semi-quantification of Er-α (n=6) and Er-β (N=6) were carried out by qPCR:.* $p<0.05$ **, $p<0.01$, *** $p<0.001$ and **** $p<0.0001$

D. Role of an AhR agonist (TCDD): Protein quantification was carried out for Er-α (long isoform, 66kDA) and were normalized to actin level and non-treated condition (n=7) : * $p<0.05$ **, $p<0.01$, *** $p<0.001$ and **** $p<0.0001$

283x181mm (300 x 300 DPI)

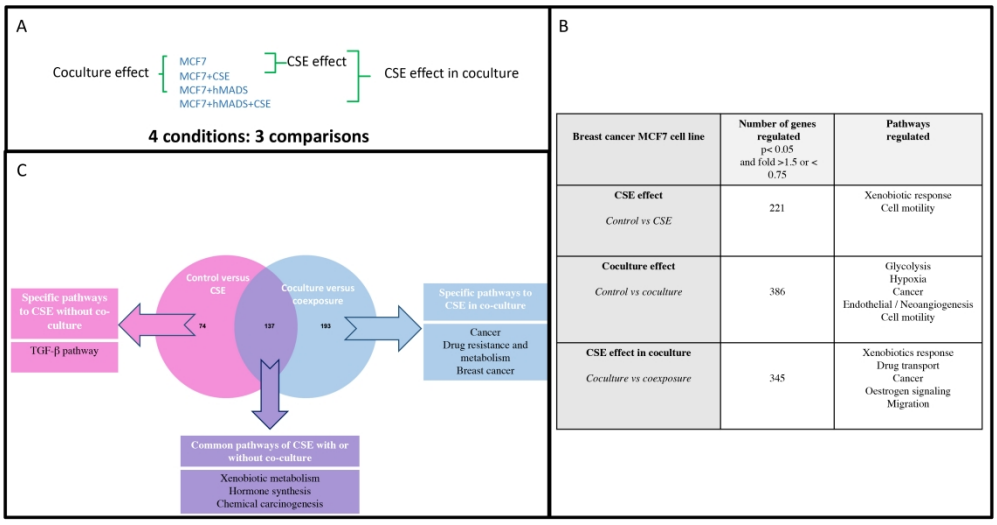

B

Breast cancer MCF7 cell line	Number of genes regulated p< 0.05 and fold >1.5 or < 0.75	Pathways regulated
CSE effect *Control vs CSE*	221	Xenobiotic response Cell motility
Coculture effect *Control vs coculture*	386	Glycolysis Hypoxia Cancer Endothelial / Neoangiogenesis Cell motility
CSE effect in coculture *Coculture vs coexposure*	345	Xenobiotics response Drug transport Cancer Oestrogen signaling Migration

Figure 8. Transcriptomic analysis of MCF-7 cells according to the different conditions: control cells, treatment by cigarette smoke extract (CSE), coculture (hMADS) or coexposure (hMADS + CSE)
A. After RNA sequencing, a differential analysis was carried out using DESeq2 package from the R softwareShinyGo v0.75 Gene Ontology Enrichment Analysis software was used for the analysis of the signaling pathways involved using the Kyoto Encyclopedia of Genes and Genomes (KEGG) database.
B. Pathways upregulated and downregulated are presented.
C. Differential analysis of genes specifically modified by CSE in coculture or without. Venn diagram representing specific pathways to CSE without or with coculture and common pathways of CSE in both conditions (Fold >1.5 or <0.75, p<0.05, top 30 terms) using the KEGG database on ShinyGo v0.75.

331x174mm (300 x 300 DPI)